## Ambiguity of Experimental Spin Information from States with Mixed Orbital Symmetries

S. N. P. Wissing, <sup>1,\*</sup> A. B. Schmidt, <sup>1</sup> H. Mirhosseini, <sup>2,†</sup> J. Henk, <sup>3</sup> C. R. Ast, <sup>4</sup> and M. Donath <sup>1</sup> Physikalisches Institut, Westfälische Wilhelms-Universität Münster, Wilhelm-Klemm-Straße 10, 48149 Münster, Germany <sup>2</sup> Max-Planck-Institut für Mikrostrukturphysik, Weinberg 2, 06120 Halle, Germany <sup>3</sup> Institut für Physik, Martin-Luther-Universität Halle-Wittenberg, Von-Seckendorff-Platz 1, 06120 Halle, Germany <sup>4</sup> Max-Planck-Institut für Festkörperforschung, Heisenbergstraße 1, 70569 Stuttgart, Germany (Received 12 February 2014; revised manuscript received 28 May 2014; published 9 September 2014)

The spin texture of the unoccupied bands of the surface alloy Bi/Ag(111) is investigated with spin- and angle-resolved inverse photoemission and first-principles calculations. Surprisingly, the measured spin character does not always reflect the calculated spin texture of the bands. With the help of photoemission calculations within the one-step model, however, the discrepancy is traced back to the influence of the orbital symmetry of the respective states in combination with the experimental geometry. In particular, the calculations show that the spin texture of a surface band with mixed orbital symmetries may neither be recovered with s- nor p- nor unpolarized light. In general, spin information from direct or inverse photoemission experiments on electronic states with mixed orbital symmetries at spin-orbit-influenced surfaces has to be taken with a pinch of salt, while it remains reliable for states with pure symmetry.

DOI: 10.1103/PhysRevLett.113.116402 PACS numbers: 71.70.Ej, 73.20.At, 79.60.-i

Angle-resolved photoemission (PE) and its time-reversed pendant, inverse photoemission (IPE) [1], are the most versatile tools for band-structure mapping  $E(\mathbf{k}_{\parallel})$  below and above the Fermi level  $E_{\rm F}$ . Since the spin is preserved in the electric dipole transition (at least to first order), spin resolution adds another quantity to the experimental information. In materials, in which the spin dependence of the band structure is dominated by exchange interaction, the electron spins are aligned perfectly either parallel or antiparallel to the quantization axis of the sample, i.e., the magnetization direction in a ferromagnet. Here, spin-resolved PE and IPE experiments can easily extract the spin character, minority or majority, of the electronic states [2].

As soon as spin-orbit interaction plays a significant role, the spin direction may depend on position in real and momentum space, as well as on the symmetry of the states. Even the spin polarization of a single electronic state may be less than one, since the spin is no longer a good quantum number in such a system. Especially at surfaces where inversion symmetry is always broken, strong spin-orbit interaction leads to a wealth of interesting spin textures in real and reciprocal space, e.g., Skyrmions [3,4], Rashba systems [5–7], and topological insulators [8,9].

Here, spin-resolved PE and IPE face a new challenge. The experimental geometry, such as the light polarization and its incidence or emission angle, influence the measured spin polarization in both magnitude and direction [10]. Spin-orbit interaction mixes states with different spin and orbital character, and the light polarization selects the orbital character of the electronic states involved in the photoemission process. Hence, the spin polarization of the photoelectron can, in principle, even be controlled

[11–16]. Indeed, it was recently reported that the measured spin polarization of electrons photoexcited from the topological surface state on  $\rm Bi_2Se_3$  is reversed by switching the light polarization from s to p [17]. This effect was attributed to relativistic corrections of the dipole operator, which allows optical spin-flip transitions [17,18].

These findings raise the general question, whether the spin information obtained in spin-resolved PE and IPE experiments provides a reliable measure of the spin character of the electronic states under investigation [19]. As a test case to answer this question, we studied the surface alloy Bi/Ag(111), known for its giant spinorbit-induced effects [20,21]. An sp<sub>z</sub> occupied surface band disperses downwards in energy [20,21] with a large conventional Rashba spin splitting [22], i.e., with spinpolarization direction in the surface plane perpendicular to  $\mathbf{k}_{\parallel}$  and antiparallel for the two branches of the spin-split state [23]. In the unoccupied part of the surface-projected band gap, theory predicts a  $p_{xy}$  surface state derived from the p states of Bi. It is, moreover, spin-orbit split into an  $m_i = 1/2$  and an  $m_i = 3/2$  state [24]. Remarkably, the two branches of the  $m_i = 1/2$  band show mainly parallel spin directions along the high-symmetry lines of the surfaceprojected Brillouin zone. This deviation from the conventional Rashba spin texture results from hybridization of states with different orbital character [25,26]. Scanning tunneling spectroscopy measurements of standing waves confirm the dispersion of the  $m_i = 1/2$  band above  $E_{\rm F}$ [27,28]. However, the standing wave data are interpreted in terms of a conventional Rashba spin texture in Ref. [28].

In the present work, we use spin- and angle-resolved IPE [7,29,30] as well as first-principles calculations to investigate the unoccupied surface electronic structure of

Bi/Ag(111). We find that, for the  $m_j=1/2$  band with mixed orbital symmetries, the measured spin information does not agree with the calculated spin polarization of the surface band. For the  $m_j=3/2$  band with almost pure orbital symmetry, however, the experimental spin information reflects the band spin polarization as in the case of the occupied surface band with  $sp_z$  symmetry. In particular, the experimental results for all surface bands on Bi/Ag(111) can be well understood without assuming spin-flip transitions.

Our spin-resolved IPE measurements were performed at room temperature using spin-polarized electrons emitted from a GaAs photocathode [31]. The angular divergence  $\Delta\theta=\pm2^\circ$  of the electron beam corresponds to a momentum resolution at  $E_{\rm F}$  of  $\Delta k_{\parallel,\rm F}=\pm0.04~{\rm \AA}^{-1}$ . The spin-up (spin-down) direction of the incident electrons, their inplane wave vector  ${\bf k}_{\parallel}$  and the surface normal  ${\bf n}$  form a right-handed (left-handed) coordinate system as shown in the inset of Fig. 1. In this geometry, the Rashba component

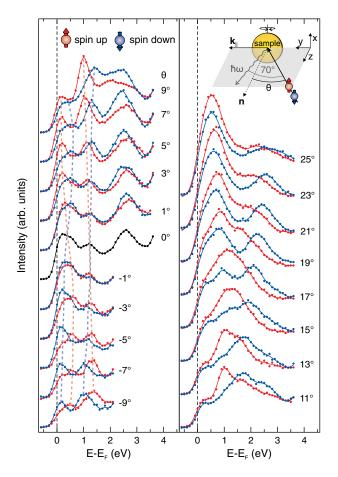


FIG. 1 (color online). Spin-resolved IPE spectra for various angles of electron incidence  $\theta$  along  $\bar{\Gamma}\bar{K}$  of the alloy surface Brillouin zone. Data points represent spin-integrated (black), spin-up (red), and spin-down (blue) intensities. Solid lines serve as guide to the eye. In the inset, a sketch of the experimental setup is given, which is sensitive to the Rashba component of the spin polarization.

of the spin polarization is measured. The photons are detected with an energy-selective Geiger-Müller counter ( $\hbar\omega = 9.8$  eV [32]) at a fixed angle of 70° with respect to the incident electron beam. The polarization of the emitted vacuum-ultraviolet light is not analyzed. The overall energy resolution  $\Delta E$  of the experiment is 350 meV.

The Ag(111) substrate was cleaned with several cycles of sputtering and annealing. One third of a monolayer of Bi atoms was deposited by molecular beam epitaxy at a substrate temperature of 575 K. The Bi atoms form a long-range ordered  $(\sqrt{3} \times \sqrt{3})R30^{\circ}$  substitutional surface alloy, verified with low-energy electron diffraction.

Electronic-structure calculations have been performed within the local density approximation to density-functional theory [33], using relativistic multiple-scattering theory as formulated in the Korringa-Kohn-Rostoker approach [34]. Solving the Dirac equation, spin-orbit coupling is accounted for in a nonperturbative manner. The semi-infinite Bi/Ag(111) system comprises three regions: bulk, surface, and vacuum. The geometric relaxation at the surface has been adopted from computations with the VIENNA *ab initio* simulation package (VASP) [35] and is in agreement with low-energy electron diffraction measurements [36,37]. From the layer-diagonal part of the Korringa-Kohn-Rostoker Green function, we compute the layer-dependent spectral density, using a broadening of 0.025 eV typical for this kind of computation [20].

In addition, we performed direct and inverse photoemission calculations within the one-step model. They include effects of the dipole transition, i.e., selection rules and matrix elements, but no spin-flip transitions [34]. Taking into account the spin-flip term in the photoemission calculation induces negligibly small corrections to the spin polarization of the photoelectrons, as expected from a perturbation of the order of  $1/c^2$ .

The spin-resolved IPE spectra are presented in Fig. 1. From the peak positions we deduce  $E(k_{\parallel})$ , shown in Fig. 2(a). Three main features are identified:

- (i) The first peak just above  $E_{\rm F}$  is attributed to the  $m_j=1/2$  state [38]. It resembles a conventional Rashbasplit band with downward dispersion. For positive  $k_{\parallel}$  the upper branch shows spin-down and the lower branch spin-up polarization and vice versa for negative  $k_{\parallel}$ .
- (ii) The second structure at 1.2 eV at  $\bar{\Gamma}$  results from the  $m_j=3/2$  band. The spin polarization of the two branches is similar to that of the  $m_j=1/2$  band. We find a large Rashba splitting, with the minimum of the spin-up branch at  $k_{\parallel}\approx 0.2~{\rm Å}^{-1}$  approximately 250 meV lower in energy than at the  $\bar{\Gamma}$  point. From there, the state disperses steeply upwards and can be followed almost to the edge of the surface Brillouin zone.
- (iii) The third structure, dispersing downwards from 2.6 eV at  $\bar{\Gamma}$ , is identified as a Ag(111) surface-umklapp band induced by the  $(\sqrt{3} \times \sqrt{3})$  reconstruction, with contributions from d bands in the vicinity of the  $\bar{\Gamma}$  point.

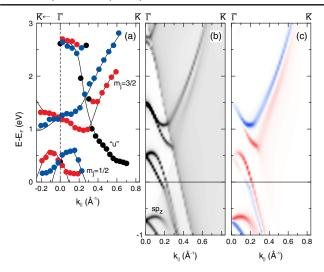


FIG. 2 (color online). Surface electronic structure of Bi/Ag(111). (a) Energy vs  $k_{\parallel}$  dispersion as derived from the IPE data in Fig. 1. The color code is identical to that in Fig. 1. Experimental uncertainties are smaller than the symbol size. (b) Calculated spectral function  $n(E,k_{\parallel})$ . Surface states appear as dark features while the bulk-derived states appear as light gray regions. (c) Difference  $n_{\uparrow}(E,k_{\parallel})-n_{\downarrow}(E,k_{\parallel})$  of the spin-projected spectral densities, indicated in red (blue) where spin-up (spin-down) intensity exceeds (white is for zero difference).

In Fig. 2(b) the calculated spectral density  $n(E, k_{\parallel})$  is depicted along  $\bar{\Gamma} \bar{K}$ . Above  $E_{\rm F}$ , the  $m_j=1/2$  and the  $m_j=3/2$  band dominate. Their dispersions are in agreement with the experiment. The band-gap edge of Ag(111), back-folded by the surface reconstruction, is visible as well. In addition, an upward dispersing band with d character appears at 2.75 eV at  $\bar{\Gamma}$ . Below  $E_{\rm F}$ , the spectral function shows the downward dispersing  $sp_z$  state.

The difference  $n_{\uparrow}(E,k_{\parallel}) - n_{\downarrow}(E,k_{\parallel})$  of the spinprojected spectral densities is shown in Fig. 2(c). The spin texture of the  $m_j = 1/2$  and  $m_j = 3/2$  bands confirms former theoretical findings [24]. The spin structure of the occupied  $sp_z$  band and the unoccupied  $m_j = 3/2$  band are in agreement with PE measurements [22] and our IPE data, respectively. However, the spin texture in the unoccupied  $m_j = 1/2$  band is at variance with our experimental results.

To resolve this problem, the calculated spin-integrated PE and IPE intensities and the spin differences  $I_{\uparrow}(E,k_{\parallel}) - I_{\downarrow}(E,k_{\parallel})$  are depicted in Fig. 3 for (a) p-polarized, (b) s-polarized, and (c) the incoherent superposition of p- and s-polarized light, i.e., unpolarized light. The  $sp_z$ ,  $m_j = 1/2$ , and  $m_j = 3/2$  bands are found in the calculated spectra, as well as the umklapp band, which crosses the  $m_j = 3/2$  band at around 1 eV.

The spin-integrated intensity is reduced when switching from p- to s-polarized light. While the intensity of the occupied  $sp_z$  band nearly vanishes (reduced by  $\approx 94\%$ ) for s-polarized light, the reduction is smaller ( $\approx 25\%$ ) for the unoccupied bands. The spin differences for the different

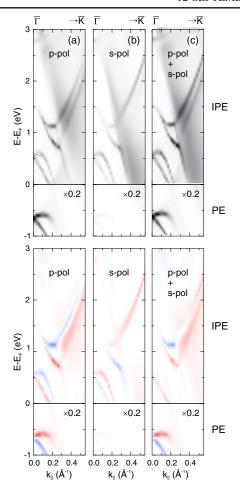


FIG. 3 (color online). Calculated spin-integrated PE and IPE intensities (upper row) and differences of the spin-resolved intensities  $I_{\uparrow}(E,k_{\parallel})-I_{\downarrow}(E,k_{\parallel})$  (lower row) for (a) p-polarized, (b) s-polarized, and (c) unpolarized light (p-pol + s-pol).

light polarizations reveal an inversion of the spin polarization for all occupied and unoccupied bands when switching from p- to s-polarized light. This is comparable to the behavior found for the topological surface state on Bi<sub>2</sub>Se<sub>3</sub> [17,18] and the Dirac-cone-like surface state on W(110) [16].

For the occupied  $sp_z$  band, the spin texture for p-polarized and unpolarized light is the same, since the intensity for s-polarized light is very small. The spin structure is in good agreement with spin-resolved photoemission measurements with p-polarized light [22]. The measured and calculated spin polarization of the photoelectrons reflects, moreover, the spin polarization found in the electronic structure calculation.

For the unoccupied bands the situation differs. The measured spin textures of the  $m_j=1/2$  and  $m_j=3/2$  bands resemble the IPE calculation for p-polarized light. However, it does not fully reproduce the calculated spin texture of the spectral function [Fig. 2(c)]. For the  $m_j=3/2$  band the experimental information reflects the band spin polarization, while for the  $m_j=1/2$  band, there

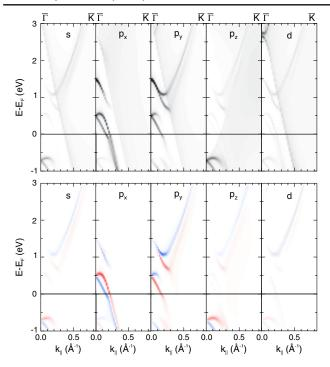


FIG. 4 (color online). Orbital decomposition of the spin-integrated (upper row) and spin-projected (lower row) spectral densities from the spectral function shown in Figs. 2(b) and 2(c). x, y, and z directions as defined in Fig. 1.

is no experimental match with the IPE calculations for s-, p-, or for unpolarized light.

To understand this discrepancy, we take a closer look at the orbital characters of the electronic states. Therefore, in Fig. 4 we present the spectral densities decomposed into s,  $p_x$ ,  $p_y$ ,  $p_z$ , and d contributions. The occupied band has almost pure  $sp_z$  orbital character. The unoccupied surface states, however, have mixed orbital symmetries of  $p_x$  and  $p_y$  character with different weights. While  $p_y$  dominates for the  $m_j = 3/2$  band, both  $p_x$  and  $p_y$  are present in the  $m_j = 1/2$  band. Pure states of  $sp_z$  and  $p_y$  character are expected to appear in spectra with  $p_y$  polarization of the light, states of  $p_x$  character with  $p_y$  polarization [41].

For the occupied  $sp_z$  band the result can be understood the easiest. This band consists almost exclusively of  $sp_z$  orbital contributions. Therefore, it can be excited with p-polarized light only, as shown in Fig. 3(a). Additionally, all orbital contributions have the same spin polarization (cf. Fig. 4). As a consequence, either p-polarized or unpolarized light will lead to a spin polarization of the photoelectrons that corresponds to the spin polarization of the  $sp_z$  band.

For the unoccupied  $p_{xy}$  bands the two main contributions come from  $p_x$  and  $p_y$  orbitals. Considering that the two orbitals also have opposite spin character [25], p or s polarization can be used to probe either one of the spin textures. As  $p_y$  prevails for the  $m_j = 3/2$ , the IPE calculation for unpolarized light is dominated by the spin texture

of the  $p_y$  orbital, which is in agreement with our experimental result. For the  $m_j = 1/2$  band the situation is more complicated. The contributions of the  $p_x$  and  $p_y$  orbitals are comparable and the band can be likewise measured with p- and s-polarized light. This leads to a situation, where the spin polarization of the electronic states is not reflected in the IPE calculation for s-, p-, or for unpolarized light.

Since our experiment does not resolve the light polarization, one might ask why our measurement resembles the spin structure computed for p-polarized light rather than unpolarized light. The calculated spin polarization depends delicately on the ratio of the different orbital contributions. Small deviations in the calculated energetic positions and dispersions of the initial and final states can modify the dipole-transition probabilities sufficiently to change the intensity ratio for p to s polarization. For example, the computed  $m_i = 3/2$  state is about 0.3 eV higher in energy than its measured equivalent [42]. Additionally, the light polarization directly at the metallic surface does not necessarily correspond to purely p- or spolarized light, which is not accounted for in the calculation. From an experimental point of view, the photon detection angle (in our case fixed at 70° in the scattering plane) influences the ratio between s- and p-polarized light contributing to the spectrum.

In conclusion, the spin information deduced from a direct or inverse photoemission experiment does not necessarily reflect the spin texture of the electronic states under investigation. Our study of the prototypical Rashba system Bi/Ag(111) serves as a test case, providing three surface bands with different symmetries. The experimental findings have been discussed along with theoretical results for the spectral functions as well as PE and IPE intensities, without assuming spin-flip transitions. In general, spin information on electronic states with mixed orbital symmetries at spin-orbit-influenced surfaces has to be taken with a grain of salt, while it remains reliable for states with pure symmetry.

It is a pleasure to thank P. Krüger for fruitful discussions.

<sup>\*</sup>Corresponding author.

Sune.Wissing@uni-muenster.de

<sup>&</sup>lt;sup>†</sup>Present address: Institute of Inorganic and Analytical Chemistry, Johannes Gutenberg University, Saarstraße 21, 55122 Mainz, Germany.

<sup>[1]</sup> J. B. Pendry, J. Phys. C 14, 1381 (1981).

<sup>[2]</sup> J. Stöhr and H. C. Siegmann, Magnetism—From Fundamentals to Nanoscale Dynamics, Springer Series in Solid-State Sciences, Vol. 152 (Springer-Verlag, Berlin, 2006).

<sup>[3]</sup> M. Bode, M. Heide, K. von Bergmann, P. Ferriani, S. Heinze, G. Bihlmayer, A. Kubetzka, O. Pietzsch, S. Blügel, and R. Wiesendanger, Nature (London) 447, 190 (2007).

<sup>[4]</sup> S. Heinze, K. von Bergmann, M. Menzel, J. Brede, A. Kubetzka, R. Wiesendanger, G. Bihlmayer, and S. Blügel, Nat. Phys. 7, 713 (2011).

- [5] S. LaShell, B. A. McDougall, and E. Jensen, Phys. Rev. Lett. 77, 3419 (1996).
- [6] M. Hoesch, M. Muntwiler, V. N. Petrov, M. Hengsberger, L. Patthey, M. Shi, M. Falub, T. Greber, and J. Osterwalder, Phys. Rev. B 69, 241401 (2004).
- [7] S. N. P. Wissing, C. Eibl, A. Zumbülte, A. B. Schmidt, J. Braun, J. Minár, H. Ebert, and M. Donath, New J. Phys. 15, 105001 (2013).
- [8] M. Z. Hasan and C. L. Kane, Rev. Mod. Phys. 82, 3045 (2010).
- [9] X.-L. Qi and S.-C. Zhang, Rev. Mod. Phys. 83, 1057 (2011).
- [10] J. Henk, T. Scheunemann, S. V. Halilov, and R. Feder, J. Phys. Condens. Matter 8, 47 (1996).
- [11] U. Fano, Phys. Rev. 178, 131 (1969).
- [12] D. T. Pierce and F. Meier, Phys. Rev. B 13, 5484 (1976).
- [13] J. Kessler, *Polarized Electrons*, 2nd ed. (Springer, Berlin, 1985).
- [14] E. Tamura, W. Piepke, and R. Feder, Phys. Rev. Lett. 59, 934 (1987).
- [15] U. Heinzmann and J. H. Dil, J. Phys. Condens. Matter 24, 173001 (2012).
- [16] H. Mirhosseini, M. Flieger, and J. Henk, New J. Phys. 15, 033019 (2013).
- [17] C. Jozwiak, C.-H. Park, K. Gotlieb, C. Hwang, D.-H. Lee, S. G. Louie, J. D. Denlinger, C. R. Rotundu, R. J. Birgeneau, Z. Hussain, and A. Lanzara, Nat. Phys. 9, 293 (2013).
- [18] C.-H. Park and S. G. Louie, Phys. Rev. Lett. 109, 097601 (2012).
- [19] J. Osterwalder, J. Phys. Condens. Matter 24, 171001 (2012).
- [20] C. R. Ast, J. Henk, A. Ernst, L. Moreschini, M. C. Falub, D. Pacilé, P. Bruno, K. Kern, and M. Grioni, Phys. Rev. Lett. 98, 186807 (2007).
- [21] H. Bentmann, F. Forster, G. Bihlmayer, E. V. Chulkov, L. Moreschini, M. Grioni, and F. Reinert, Europhys. Lett. 87, 37003 (2009).
- [22] F. Meier, H. Dil, J. Lobo-Checa, L. Patthey, and J. Osterwalder, Phys. Rev. B 77, 165431 (2008).
- [23] Yu. A. Bychkov and E. I. Rashba, JETP Lett. 39, 78 (1984).
- [24] G. Bihlmayer, S. Blügel, and E. V. Chulkov, Phys. Rev. B 75, 195414 (2007).

- [25] H. Mirhosseini, J. Henk, A. Ernst, S. Ostanin, C.-T. Chiang, P. Yu, A. Winkelmann, and J. Kirschner, Phys. Rev. B 79, 245428 (2009).
- [26] H. Bentmann, S. Abdelouahed, M. Mulazzi, J. Henk, and F. Reinert, Phys. Rev. Lett. 108, 196801 (2012).
- [27] H. Hirayama, Y. Aoki, and C. Kato, Phys. Rev. Lett. 107, 027204 (2011).
- [28] L. El-Kareh, P. Sessi, T. Bathon, and M. Bode, Phys. Rev. Lett. 110, 176803 (2013).
- [29] M. Donath, J. Phys. Condens. Matter 11, 9421 (1999).
- [30] S. D. Stolwijk, A. B. Schmidt, M. Donath, K. Sakamoto, and P. Krüger, Phys. Rev. Lett. **111**, 176402 (2013).
- [31] U. Kolac, M. Donath, K. Ertl, H. Liebl, and V. Dose, Rev. Sci. Instrum. 59, 1933 (1988).
- [32] M. Budke, V. Renken, H. Liebl, G. Rangelov, and M. Donath, Rev. Sci. Instrum. 78, 083903 (2007).
- [33] J. P. Perdew and Y. Wang, Phys. Rev. B 45, 13244 (1992).
- [34] J. Henk, in *Handbook of Thin Film Materials*, Vol. 2, edited by H. S. Nalwa (Academic, New York, 2002) Chap. 10, p. 479.
- [35] G. Kresse and J. Furthmüller, Comput. Mater. Sci. 6, 15 (1996); Phys. Rev. B 54, 11169 (1996).
- [36] I. M. McLeod, V. R. Dhanak, A. Matilainen, M. Lahti, K. Pussi, and K. H. L. Zhang, Surf. Sci. 604, 1395 (2010).
- [37] I. Gierz, B. Stadtmüller, J. Vuorinen, M. Lindroos, F. Meier, J. H. Dil, K. Kern, and C. R. Ast, Phys. Rev. B 81, 245430 (2010).
- [38] The remaining intensity measured for the  $m_j = 1/2$  state for  $k_{\parallel} > 0.1 \text{ Å}^{-1}$  is a consequence of the limited momentum resolution in combination with the Fermi distribution at room temperature and the intrinsic line width of the surface state [39,40]. Spectral features appearing closer to  $E_F$  than the experimental energy resolution do not necessarily coincide with final-state energies.
- [39] M. Donath and V. Dose, Europhys. Lett. 9, 821 (1989).
- [40] S. D. Stolwijk, A. B. Schmidt, and M. Donath, Phys. Rev. B 82, 201412 (2010).
- [41] J. Hermanson, Solid State Commun. 22, 9 (1977).
- [42] The spin-orbit splitting of the  $m_j = 1/2$  (which fits well to the experiment) and the  $m_j = 3/2$  state are fixed by the strength of the spin-orbit coupling which is fully determined by the Dirac equation.